



3 4456 0514445 7



A COPY

OAK RIDGE NATIONAL LABORATORY

operated by

UNION CARBIDE CORPORATION
NUCLEAR DIVISIONfor the
U.S. ATOMIC ENERGY COMMISSION

ORNL-TM-3449

cy. 67

DATE - June 15, 1971

Neutron Physics Division

OPTIMIZATION OF A SHIELD FOR A HEAT-PIPE-COOLED FAST REACTOR
DESIGNED AS A NUCLEAR ELECTRIC SPACE POWER PLANT

Work Done By:

W. W. Engle, Jr.

R. L. Childs*

F. R. Mynatt

Report Written By:

W. W. Engle, Jr.

R. L. Childs*

F. R. Mynatt

Lorraine S. Abbott

ABSTRACT

A reactor shield optimization procedure based on the ASOP shield optimization computer code and the DOT radiation transport code was used to determine a minimum-weight shield for a small fast reactor designed for a space nuclear electric power plant. The reactor, cylindrical in shape, is fueled with uranium nitride and cooled by potassium circulating through a matrix of stainless steel heat pipes embedded in the core; the design power is 450 kWt. The surrounding shield is typically asymmetric, having the overall shape of a truncated 90-deg cone whose thick base is positioned between one end of the reactor and the crew compartment. The heat pipes emerge from the opposite end of the reactor, penetrating through the apex of the shield. The dose constraints are 1 mrem/hr at all 100-ft radii falling within the shadow cast by the base of the cone and 300 mrem/hr at all other 100-ft radii. The optimized shield consists of alternate layers of tungsten and lithium hydride, the thick bottom section extending out to a radius of 112 cm and the tapered side decreasing to a radius of 89 cm. The top heat-pipe shield region consists of a 59-cm-thick inner layer of a stainless-steel-BiC mixture and a 30.5-cm-thick outer layer of a BeC-BiC mixture. The total shield weight is 25,589 lb. A partially optimized shield having a 45-deg cone angle and a higher dose constraint for positions outside the cone shadow (100 rem/hr) has a total weight of 14,708 lb. These shield weights include an allocation for 3.5 vol% of stainless steel structure in the LiH regions.

*Mathematics Division.

NOTICE This document contains information of a preliminary nature and was prepared primarily for internal use of the Oak Ridge National Laboratory. It is subject to revision or correction and therefore does not represent a final report.

This report was prepared as an account of work sponsored by the United States Government. Neither the United States nor the United States Atomic Energy Commission, nor any of their employees, nor any of their contractors, subcontractors, or their employees, makes any warranty, express or implied, or assumes any legal liability or responsibility for the accuracy, completeness or usefulness of any information, apparatus, product or process disclosed, or represents that its use would not infringe privately owned rights.

TABLE OF CONTENTS

	<u>Page No.</u>
I. Introduction -----	5
II. The ASOP Technique -----	7
III. The Reactor and Its Calculational Model -----	9
IV. Preliminary Calculations for a Two-Cycle Shield with a 45-deg Cone Angle -----	10
V. Optimization of a Three-Cycle Shield with a 90-deg Cone Angle -----	20
App. A. Shield Calculations for High-Power Operation -----	35
App. B. Cross Sections Used in Calculations -----	37
References -----	39



3 4456 0514445 7

ACKNOWLEDGEMENTS

The authors wish to express appreciation to C. E. Clifford, who not only encouraged the development of the shield optimization procedure but also gave many helpful suggestions during the course of this particular application. The heat-pipe reactor concept and shield design constraints were provided by A. P. Fraas.

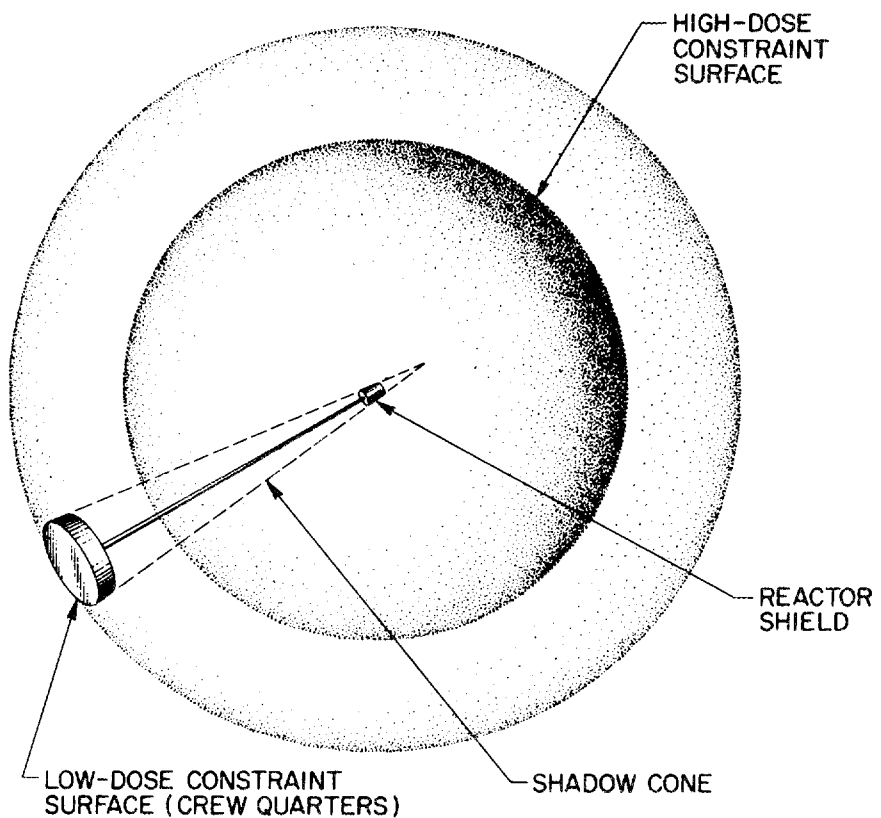
I. INTRODUCTION

A reactor shield optimization procedure based on the ASOP shield optimization code¹ and the DOT two-dimensional radiation transport code² has been used to determine a minimum-weight shield for a conceptual heat-pipe-cooled fast reactor designed by ORNL as a nuclear electric power plant for spacecraft.³ The ASOP code (ANISN Shield Optimization Program), using one-dimensional discrete ordinates transport theory and three-dimensional weight functions, has been applied previously to the optimization of shields for several U-ZrH SNAP reactors.⁴ The application of the code as described here differs from its earlier applications in two respects: the neutron spectrum in the heat-pipe reactor is harder than that in a U-ZrH reactor, and the high temperature of the heat pipes requires the design of an optimum high-temperature shield zone.

Shields for space power reactors are typically asymmetric, and the shield optimization procedure determines the thicknesses and positions of the various shield components required to meet the dose constraints with the least weight. Overall the shape of the shield surrounding the reactor is that of a truncated cone whose thick base intercepts radiation directed toward the crew compartment. Dose constraints are specified for spherical surfaces, or portions of spherical surfaces, described by constant radii from the center of the reactor, the most severe dose constraint being, of course, for the crew position. The dose constraints for other regions around the reactor are considerably higher but low enough to allow specified activities, as, for example, docking with other spacecraft. The relationship of the reactor shield, crew position, and dose constraint surfaces is illustrated in Fig. 1. Note that the crew position falls within the "shadow" cast by the bottom of the shield.

In setting the dose constraints consideration must be given to the possibility that structure will protrude outside the shadow cone outlined in Fig. 1, in which case radiation emitted from the side or top of the shield could scatter from the structure to the crew quarters. In the final shield design study described here, it was assumed that the large power conversion components (heat exchangers, turbines, and radiators for a Brayton cycle system) would extend outside the cone angle; therefore the side and top

ORNL-DWG 71-4010



NOT TO SCALE

Fig. 1. Sketch Showing Relationship of Reactor Shield, Crew Quarters, and Dose Constraint Surfaces. (Note: In some calculations the radii for the high- and low-dose constraint surfaces are the same.)

shield were designed to reduce the neutron flux to the extent that scattering from this equipment would be unimportant.

The materials used for this shield design were tungsten alloyed with molybdenum for the gamma-ray attenuation and lithium hydride for the neutron attenuation (see Table 1). Although the use of a tungsten alloy produces a heavier shield than materials such as lead or uranium would, optimization studies have shown the weight penalty to be a few percent. The benefit gained from using tungsten is that the secondary gamma-ray production cross sections needed for the design calculations have been shown to be fairly adequate and resonance self shielding is less important than for the other materials.

The lithium hydride was assumed to be contained in a stainless steel honeycomb held in a stainless steel can. Additional stainless steel was included in the LiH region to account for structural members of the engineered shield. The stainless steel represented 3.5 vol.% of the LiH region and was considered to be homogenized with the LiH in the calculation.

It will be noted from the following presentation that after the basic shield was evolved by the ASOP technique, refinements based on a series of DOT calculations of isodoses within the shield reduced the shield weight an additional 10%. This weight reduction is not nearly as dramatic as those from other applications of the shield optimization procedure using the isodose information, some of which have resulted in weight savings as large as 30%. In this case, however, the design of the basic shield itself benefitted from the experience gained in the earlier applications. Also, the cone angle specified for this particular reactor shield dictates an essentially hemispherical bottom shield which limits refinements to those portions of the shield that represent only a small fraction of the weight.

II. THE ASOP TECHNIQUE

In the ASOP program a module consisting of the one-dimensional ANISN code is used to calculate the coupled neutron and gamma-ray transport for an assumed spherical shield configuration and for each of several perturbations of that configuration in order to obtain approximations for the first and second derivatives of the total dose with respect to each design variable.

Table 1. Compositions of Principal
Shield Materials

Material	Density (atoms/barn-cm)
LiH-SS	
⁶ Li	0.0041188
⁷ Li	0.0506526
H	0.0547717
Fe	0.002068
Cr	0.0006274
Ni	0.0003816
Mo	0.0001111
W-Mo	
W	0.05972
Mo	0.002335

The geometry of the calculation includes the reactor core and thus primary gamma rays from fission as well as secondary gamma rays produced by other neutron interactions throughout the core and shield are included. The information generated in these calculations is used to solve a set of linear equations for a new set of shield dimensions. These new dimensions satisfy two conditions: (1) the dose at some point external to the shield is equal to the specified design level, and (2) the derivative of the dose with respect to weight for a differential change in each design variable is an unspecified constant. Because the new dimensions may lie outside the range of the assumed linearities, the process is repeated until the shield configuration converges.

In general, the assumed shield configuration has either two or three cycles, the number of cycles denoting the number of heavy metal layers in the shield. Survey calculations have shown that considerable weight savings is effected with each increase in the number of cycles up to three but that little is gained by introducing more than three cycles. Because calculations for two-cycle shields are presently easier and less expensive to perform than those for three-cycle shields, the optimization of a shield for a particular reactor may begin with two-cycle calculations and then change to a three-cycle configuration during the final design steps.

III. THE REACTOR AND ITS CALCULATIONAL MODEL

The heat-pipe-cooled reactor for which this study was performed consists of a right circular cylinder of fully enriched uranium nitride fuel in which a matrix of stainless steel heat pipes is embedded. The heat pipes contain potassium as the working fluid and run parallel to the axis of the core, emerging from the end of the core opposite from the crew compartment (that is, from the top of the core). A 5-in.-diam cylindrical nickel control plug moves along the axis of the core, which is surrounded by a 1.5-in.-thick niobium reflector. The reactor core size is 9.9 in. in diameter and 12 in. in height, and the design power level is 450 kWt. (A few calculations performed for a 14.5-in.-diam by 12-in.-high core and a design power of 1780 kWt are described in an appendix to this report.)

The spherical model of the reactor used in the one-dimensional ASOP calculations conserved the volumes for the control plug and core and the thickness for the niobium reflector. The representation of the reactor for the succeeding two-dimensional DOT calculations was straightforward in r-z geometry. Figure 2 shows the r-z model which was taken from reactor design calculations.⁵

Tables 2 and 3 list the volume fractions and atomic densities respectively for the reactor materials.

IV. PRELIMINARY CALCULATIONS FOR A TWO-CYCLE SHIELD WITH A 45-deg CONE ANGLE

The optimization of the shield for the reactor operating at 450 kWt was initiated with several survey-type calculations that provided the reactor designers with the variation of the approximate shield weight with the dose constraints and with the reactor-crew separation distance. In the first set of ASOP calculations the dimensions of a spherically symmetric two-cycle W-LiH shield were determined for dose constraints of 0.75, 3, and 12 mrem/hr at a distance of 200 ft from the center of a spherical model of the reactor. The results shown in Fig. 3 indicate how the thicknesses of the individual layers and the overall radius of the shield vary with the dose. These plots can also be used to determine shield thicknesses for other distances since beyond the shield surface the only attenuation of the dose is the geometric attenuation, which varies as r^2 . That is, if the shield thickness for a distance of 100 ft were desired, then for a given dose constraint the geometric attenuation would be less by a factor of four and could be compensated for by choosing dimensions for a dose constraint lower by a factor of four.

Since the reactor is to be cooled with heat pipes that emerge from the top of the 9.9-in.-diam cylindrical core and the high temperatures will preclude the use of LiH in this region, it was necessary to investigate the use of some other neutron shielding material around the heat pipes. The substitution of BeO was considered and because BeO is more dense than LiH, 2.96 g/cm³ as compared to 0.8 g/cm³, it was at first assumed that an accompanying W layer would not be required. The first ASOP calculations for this region

ORNL-DWG 71-4012

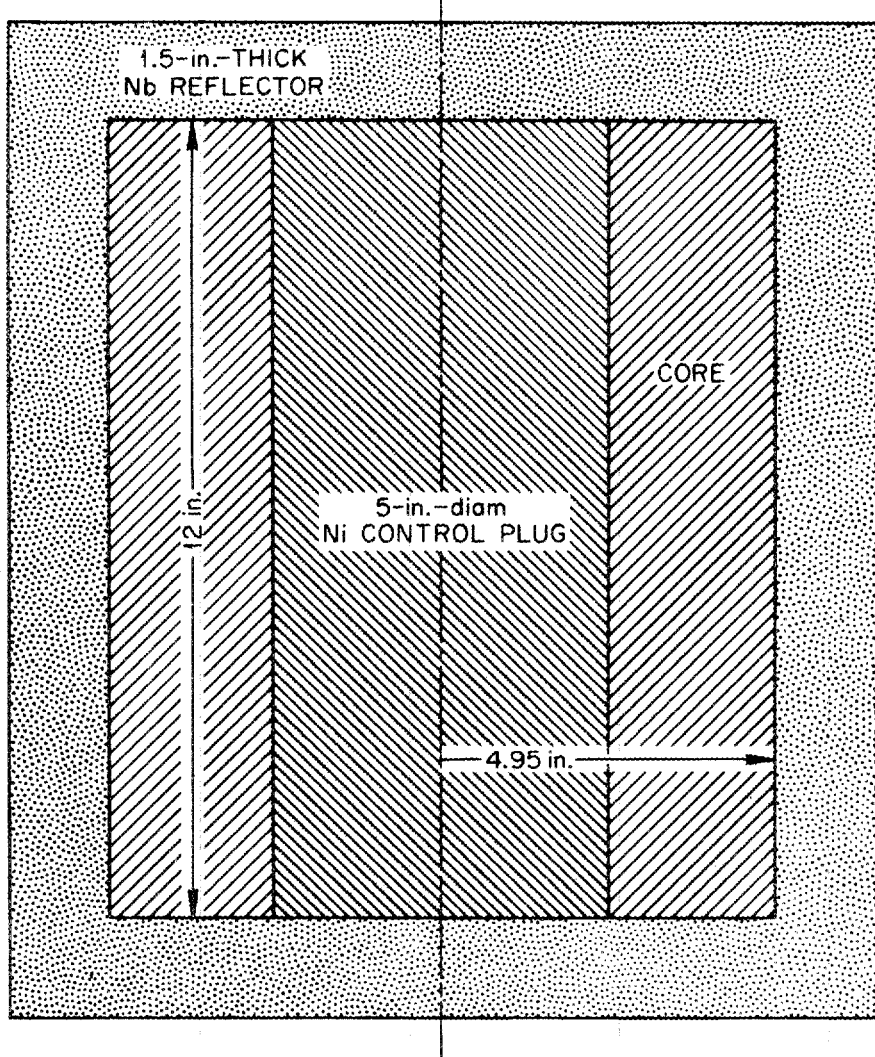


Fig. 2. Representation of Heat-Pipe-Cooled Reactor in Two-Dimensional Shield Calculations.

Table 2. Volume Fractions of Core Materials

Component	Volume Fraction for Core Power of	
	450 kWt	1780 kWt
Heat Pipes	(0.2)	(0.5)
Stainless steel	0.02868	0.0717
Potassium (liquid)	0.04862	0.1215
Potassium (vapor)	0.1227	0.3068
Uranium Nitride	0.8	0.5

Table 3. Atomic Densities of Core Materials

Material	Density (atoms/barn-cm)
Uranium nitride	
^{235}U	0.03068
^{238}U	0.00221
N	0.0329
Stainless Steel	
Fe	0.0631
Ni	0.00649
Cr	0.0165
Potassium (liquid)	0.00986
Potassium (vapor)	0.0000148
Nickel plug	0.0883
Niobium reflector	0.0545

revealed, however, that the thickness of BeO that would meet the dose constraint assumed for the side and top shield -- 1.2 rem/hr at a distance of 150 ft for this particular calculation -- was approximately 150 cm (see sketch a in Fig. 4), which is much greater than the 93-cm thickness that would be required if the shield consisted of W and LiH (see sketch c). While the weight for a thick BeO region itself is relatively unimportant compared to the total weight of the shield, an extended heat-pipe shield region would dictate additional top and side shielding to protect the crew from scattered radiation. Therefore the design criterion adopted was that the thickness of the top heat-pipe shield zone be sufficiently small that it is contained within the cone defined by a side shield that meets the side dose constraint. A second ASOP calculation was performed with an inner W layer in the heat-pipe region. As a result the radius of the region was decreased by about 43 cm, as is apparent from a comparison of sketches a and b in Fig. 4, and the 107-cm radius for the W-BeO heat-pipe shield zone is only 15% greater than that for a two-cycle W-LiH shield for the same dose constraint as shown in sketch c. For the W-BeO heat-pipe shield calculations it was assumed that the heat pipes (20 vol%) follow a spiraled pattern from the core through the shield and thus the heat-pipe materials could be homogenized with those in which they were embedded.

With W and BeO established as a suitable combination for the heat-pipe region, survey-type calculations were performed to determine the variation of the W and BeO thicknesses and the shield radius with the dose constraint. Three spherical-geometry ASOP calculations were carried out for dose constraints of 1, 10, and 100 rem/hr at a distance of 100 ft. The results presented in Fig. 5 show the variations in the shield layers with the dose.

Another set of survey-type calculations was then performed for the definition of a minimum side and top shield excluding the heat-pipe region, again for dose constraints of 1, 10, and 100 rem/hr at a distance of 100 ft. A one-cycle W-LiH material configuration was assumed and the results of the ASOP calculation, shown in Fig. 6, indicate that W would not be needed if the allowable dose rate were greater than about 17 rem/hr.

On the basis of the data presented in Figs. 3, 5, and 6 and with a total included crew-shield cone angle of 45 deg specified by the reactor designers,

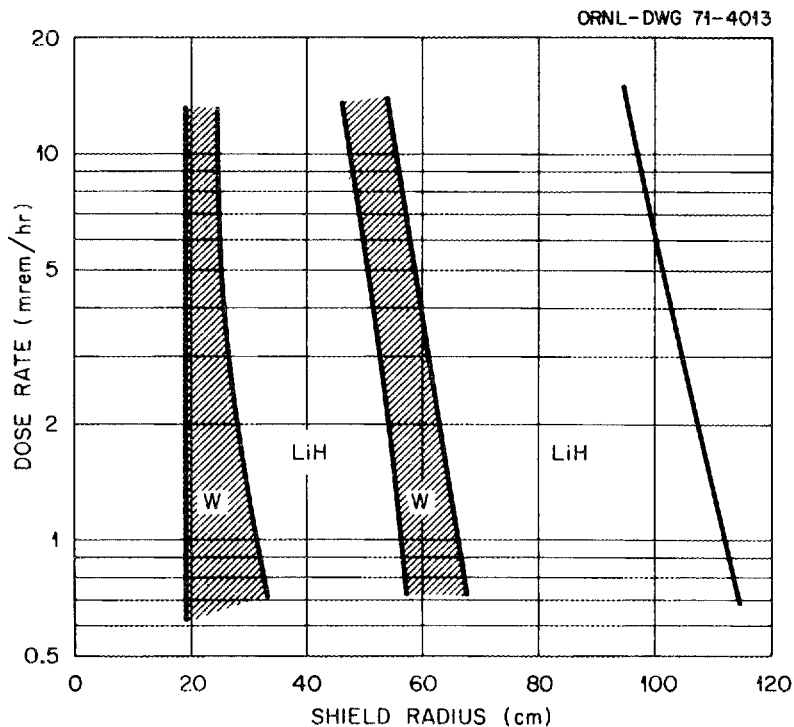


Fig. 3. Thicknesses of W and LiH Layers in a Two-Cycle Shield as a Function of Dose Rate at a Distance of 200 ft (450 kWt).

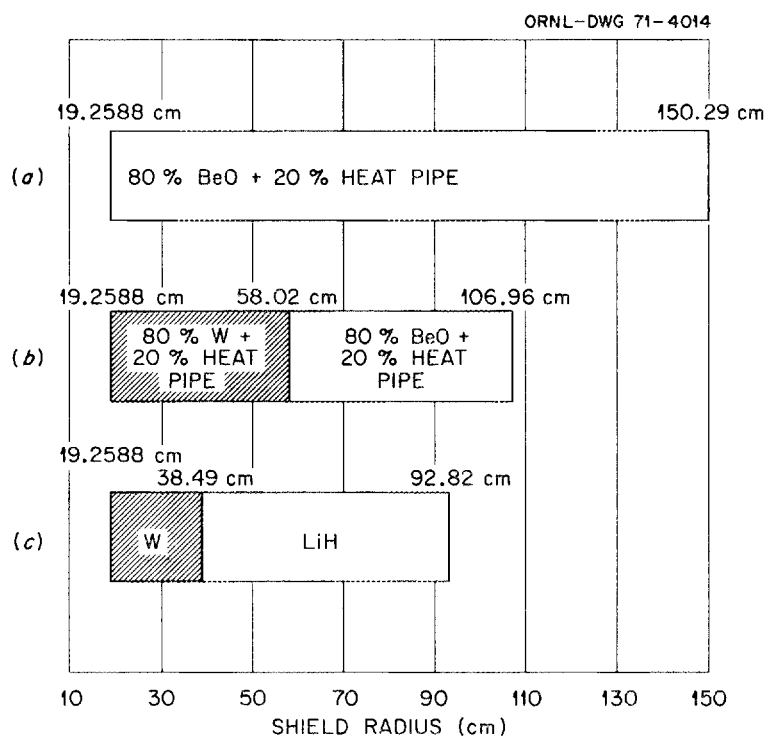


Fig. 4. Relative Thicknesses of Three Heat-Pipe Shield Configurations for a Total Dose Constraint of 1.2 rem/hr at a Distance of 150 ft (450 kWt).

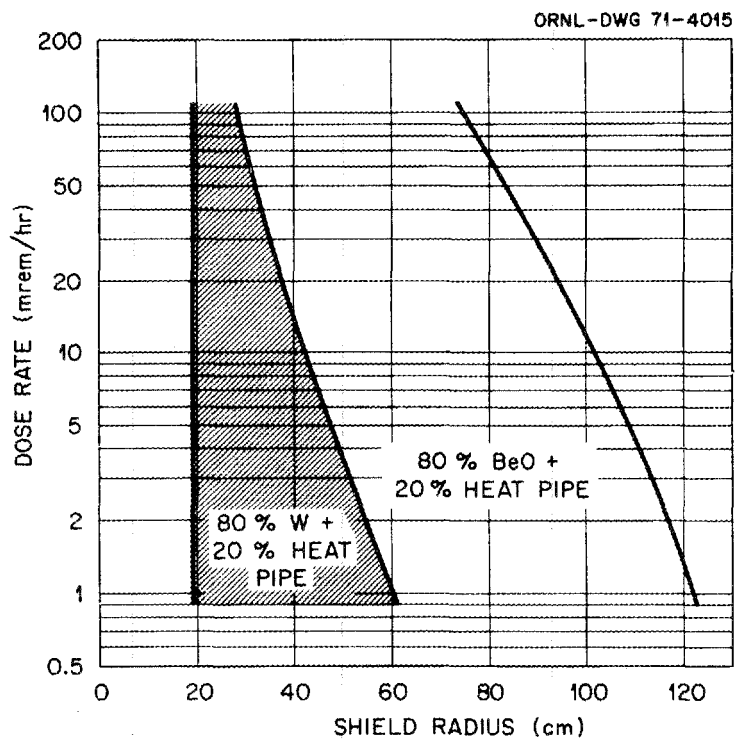


Fig. 5. Thicknesses of W and BeO Layers in Top Shield as a Function of the Dose Rate at a Distance of 100 ft (450 kWt).

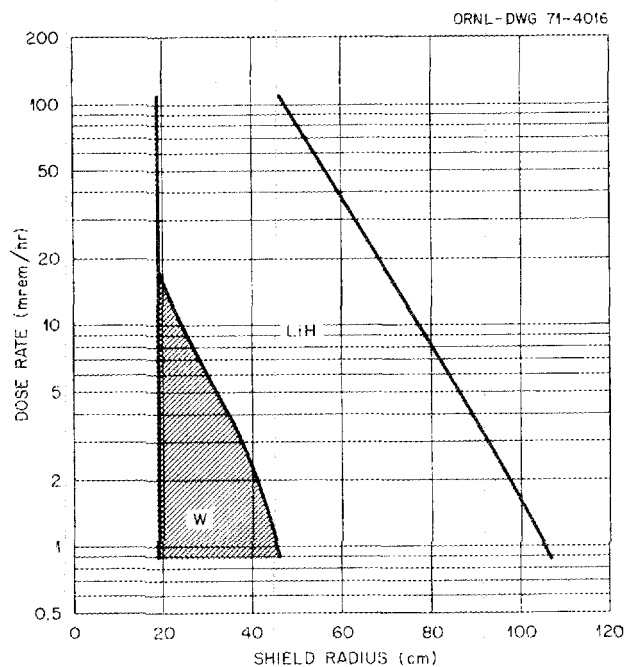


Fig. 6. Minimum Thicknesses of W and LiH Layers in Side Shield as a Function of the Dose Rate at a Distance of 100 ft (450 kWt).

the two-cycle, two-dimensional shield was designed for a reactor-crew separation distance of 100 ft, for a dose constraint of 3 mrem/hr at the crew location, and for a maximum of 100 rem/hr at the surface of a 100-ft-radius sphere around the reactor. Steps in the design included the following:

- (1) Substituting the two-dimensional reactor model for the spherical model,
- (2) Defining the shield to be a cone whose apex is truncated to coincide with the outer surface of the shielded heat-pipe region,
- (3) Setting the shield thicknesses along the reactor-crew axis as specified in Fig. 3 (a dose rate of 3 mrem/hr at 100 ft would be the same as 0.75 mrem/hr at 200 ft),
- (4) Setting the shield thicknesses in the heat-pipe region as specified in Fig. 5 for a 100 rem/hr dose rate at 100 ft,
- (5) Maintaining a minimum thickness of LiH in the region adjacent to the heat-pipe region as specified in Fig. 6 for a 100-rem/hr dose rate at 100 ft.

Except for the above specifications, the internal shape of the shield was not specified by the one-dimensional optimization; however, adjustments were made within the shield to reduce its overall weight. In particular, the outer regions of the W layers were moved to positions in which they would weigh the least while at the same time maintaining a constant thickness of each W zone and not allowing the thickness of the intervening LiH layer to fall below that along the reactor-crew axis. The resulting configuration is shown in Fig. 7.

The final step in this study of the two-cycle shield was to perform a two-dimensional DOT calculation for the complete system to determine whether the dose constraints truly had been met. The results for a constant radial distance of 100 ft are shown in Table 4 as a function of the angle measured from the reactor-crew axis at the center of the reactor.* All angles less

*For the large distance involved, measuring the angle from the center of the core instead of from the apex of the shield makes little difference in the area described by the cone at the crew position.

ORNL-DWG 71-4017

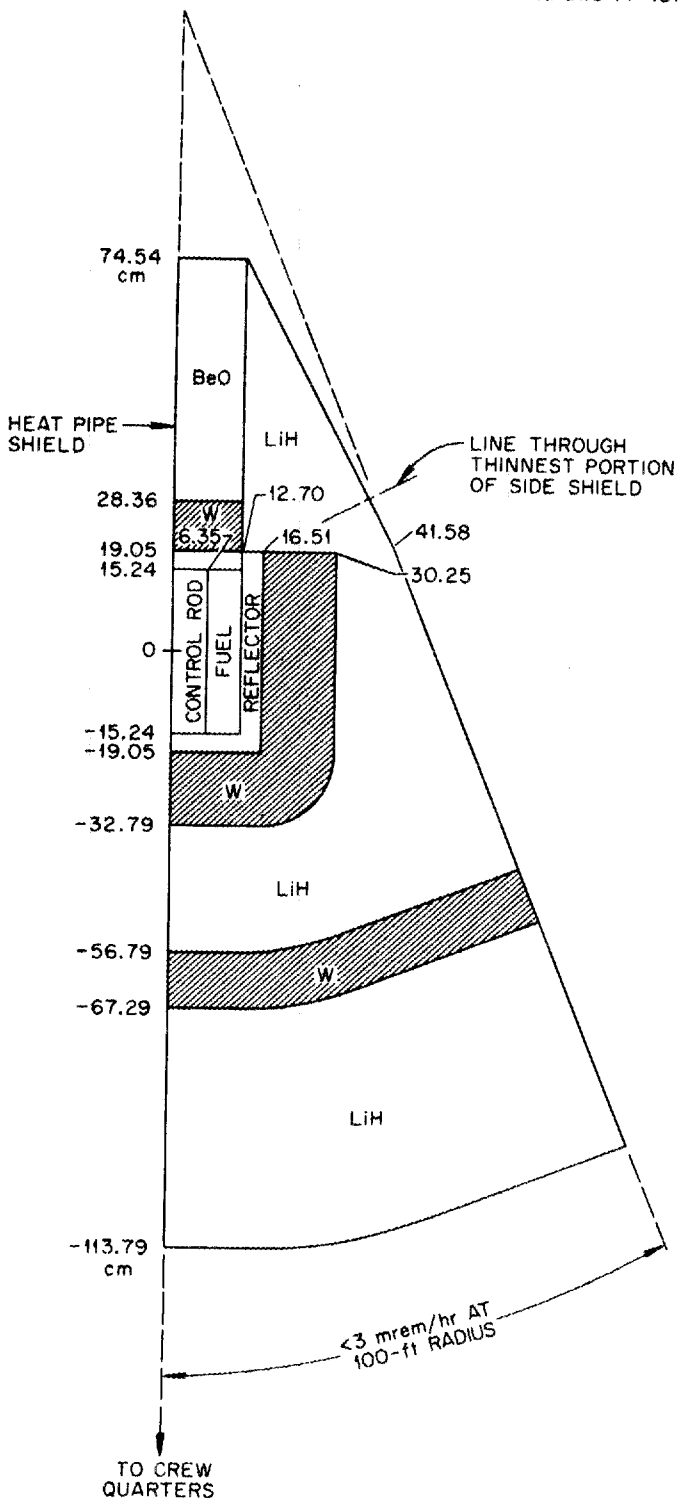


Fig. 7. Configuration for a Two-Cycle Asymmetric Shield with a 45-deg Cone Angle (450 kWt).

Table 4. Dose Rates at a Constant 100-ft Radius Around
a 14,708-lb Two-Cycle Shield with 45-deg Cone Angle^a

Angle ^a (deg)	Dose Rate (mrem/hr)
0	2.11
15	2.37
30	531
60	12995
90	29862
120	54777
150	51025
180	32188

^aMeasured from reactor-crew axis at center
of core.

than 22-1/2 deg are within the shadow cone and should have dose rates less than 3 mrem/hr, which explains the sudden jump from 2.37 mrem/hr at 15 deg to 531 mrem/hr at 30 deg. The dose rates between 30 and 180 deg are all well below the 100,000-mrem/hr dose constraint, the highest dose rate being approximately a factor of two lower than that allowed. The fact that the dose through the heat-pipe region is approximately one-third that predicted by the ASOP calculation is probably attributable to the fact that the LiH around the heat-pipe region is more effective than the BeO both in attenuating neutrons and in reducing secondary gamma-ray production. (One-dimensional calculations assume a complete spherical shell of homogenized BeO and heat pipes.)

The shield which gives the dose rates shown in Table 4 weighs 14,708 lb. Its weight could be reduced considerably (up to 30%) by tapering the tungsten layers, and possibly the LiH layers, in the side regions and performing additional DOT calculations. Also, studies for other reactors have shown that converting the shield to a three-cycle system would result in a 10 to 15% weight decrease. But at this point it had become apparent that it would be very difficult to place the power conversion equipment required for this reactor in positions that would not cause excessive scattered radiation dose rates at the crew quarters. Since, due to shielding considerations, the heat pipes must penetrate through the top of the shield, an intermediate heat exchanger must be placed beyond the top of the shield, and this heat exchanger will be relatively large because the potassium from the heat pipes will be mostly in the vapor phase. Therefore the side shield radius must be enlarged to protect the low-dose constraint zone from radiation scattered from the intermediate heat exchanger. Similarly, the final heat exchanger, together with the compressor, turbines, and radiators, must be placed below the base of the shield within the protection of the shadow cone, and the combined size of this equipment dictates a larger diameter for the base of the shield. These considerations, along with the requirements for a larger crew operating area, resulted in a shift to a 90-deg cone angle, for which the shield design is described in Section V.

V. OPTIMIZATION OF A THREE-CYCLE SHIELD WITH A 90-deg CONE ANGLE

In addition to the 90-deg cone angle, the criteria specified for the second shield designed for the heat-pipe reactor were a 100-ft reactor-crew separation distance, a maximum crew dose rate of 3 mrem/hr, and a maximum side-shield dose constraint of 100 rem/hr at a 100-ft distance. The side dose constraint was modified, however, when it was decided that the shield would be designed to allow placement of power conversion equipment outside the cone angle and that the radiation scattered therefrom to the crew quarters should not exceed 3 mrem/hr. With an arbitrary factor of 100 allowed for scattering, the side dose constraint was then reduced to a maximum of only 300 mrem/hr at 100 ft. Using this specified dose criterion, an ASOP calculation was performed for a three-cycle W-LiH shield. The results of this calculation determined the W-LiH configuration along the axis between the reactor and crew.

Although the calculations that had already been performed for the heat-pipe region of the shield were independent of the number of cycles used in the remainder of the shield, the new dose constraint of 300 mrem/hr was not within the range of data given in Fig. 5, necessitating additional ASOP calculations. For these spherical heat-pipe shield calculations the dose criterion of 300 mrem/hr was specified for neutrons only. This decision was justified on the basis that only neutrons would be likely to negotiate the large angle of scattering from the power conversion equipment above the heat-pipe zone to the crew location. Also, the two-cycle studies had shown that when the DOT calculations were performed for the complete system, the LiH surrounding the heat-pipe region reduced the dose at the 180-deg angle well below that indicated by the ASOP calculation, thus allowing for the additional dose rate from gamma rays.

Several heat-pipe shield materials were considered, and an ASOP calculation was performed for each case. The resulting configurations are depicted in Fig. 8. In each case the heat-pipe materials (20 vol%) were homogenized with the shield materials in the calculational model. The first material calculated was B₄C. The resulting thickness was too great -- about 10 cm thicker than the three-cycle crew shield. Because iron has a

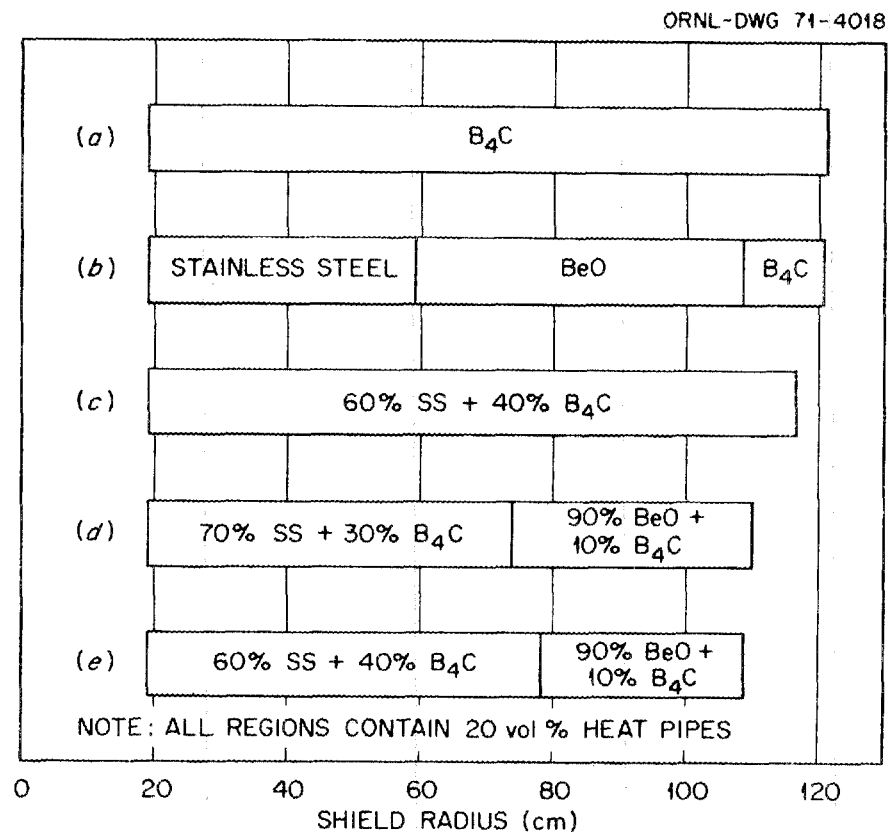


Fig. 8. Relative Thicknesses of Five Heat-Pipe Shield Configurations for a Neutron Dose Constraint of 300 mrem/hr at a Distance of 100 ft (450 kWt).

high cross section for fast-neutron inelastic scattering, and beryllium and boron are effective shield materials for intermediate and thermal energy neutrons, a configuration of individual layers of stainless steel, BeO, and B₄C was then used. Disappointingly, the thickness remained approximately the same as that for B₄C alone. Next a mixture of 60% stainless steel and 40% B₄C was tried, again with little improvement in thickness. Finally a mixture of stainless steel and B₄C followed by a mixture of BeO and B₄C was used, yielding a thickness approximately the same as that of the three-cycle crew shield. Varying the relative percentages of the stainless steel and B₄C gave a slight further improvement, and this last configuration was chosen for the final design. Note that in each case ASOP determined the zone thicknesses and each result is a relative optimum for the given materials. The compositions of the materials in the heat-pipe region are given in Table 5.

With the materials and thicknesses of the top and bottom sections of the shield determined and the cone angle of 90 deg specified, the approximate shape and composition of the asymmetric shield around the real reactor became apparent. Before the final shield could be designed, however, it was necessary to define the minimum permissible side shield (that is, the shield along a perpendicular from the side shield surface to a top corner of the reactor). This was done with one further ASOP calculation performed for a three-cycle W-LiH shield and a dose constraint (neutrons plus gamma rays) of 300 mrem/hr at a radius of 100 ft. In this calculation the inside surfaces of the W layers were fixed at the same radii determined for the bottom section of the shield to ensure that the bottom and side sections would blend together. The results revealed that a two-cycle shield would suffice for the side shield, and further that one of the remaining W layers could be made thinner. (ASOP eliminates a cycle by reducing one of the heavy-metal layers to an infinitesimal thickness, in this case the outer layer.) The final thicknesses of materials in the side shield are shown in sketch b of Fig. 9. These are to be compared with the thicknesses determined earlier for the bottom shield (sketch a) and the top shield (sketch c).

Table 5. Composition of Materials in Heat-Pipe
Shield Region

Material	Density (atoms/barn-cm)
SS-B ₄ C	
Fe	0.0337
Cr	0.0102
Ni	0.0062
Mo	0.0018
B	0.0443
C	0.0111
BeO-B ₄ C	
Be	0.0513
O	0.0513
B	0.0089
C	0.022

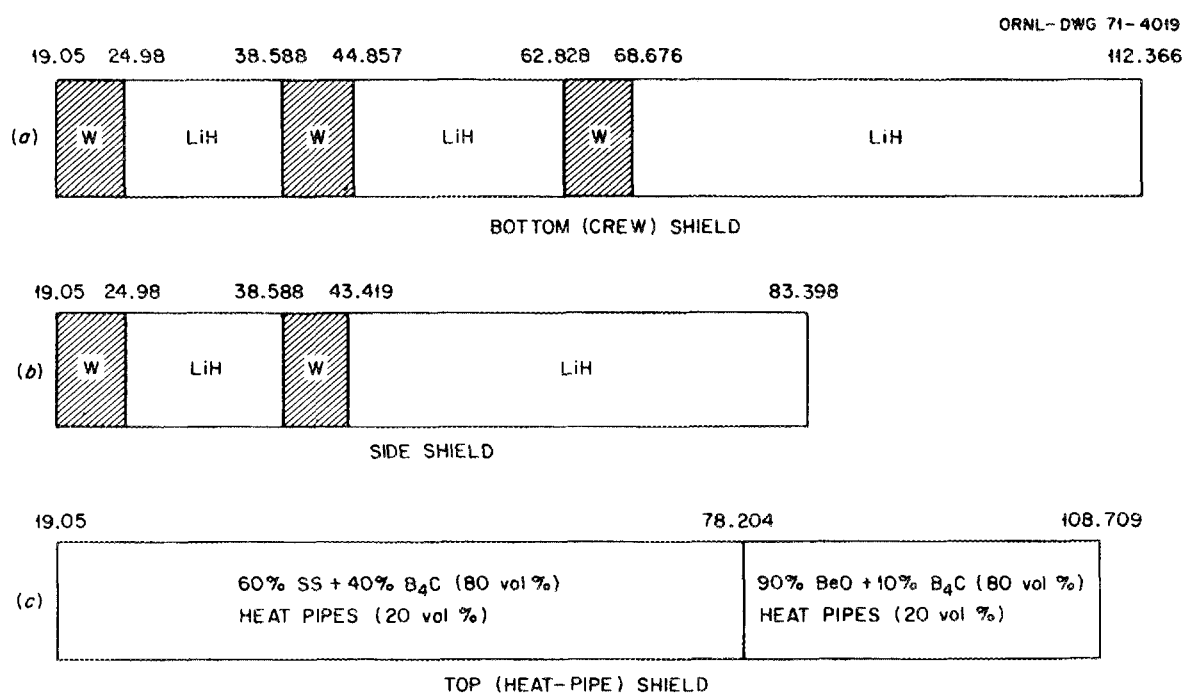


Fig. 9. Shield Thicknesses Indicated by ASOP Calculations for Bottom, Side, and Top Shields (Three-Cycle Shield with 90-deg Cone Angle).

On the basis of all the preceding calculations the shield design shown in Fig. 10 evolved. Note that the outer layer of W is terminated where it enters the side shield. The total weight of the shield is 28,305 lb.

When the shield shown in Fig. 10 was checked by a two-dimensional DOT calculation, it yielded total dose rates at a constant 100-ft radial distance as shown in Table 6. All doses for angles less than 45 deg are below the dose constraint of 3 mrem/hr, and those for angles greater than 45 deg are below the dose constraint of 300 mrem/hr except at an angle of 150 deg, which corresponds to the thinnest portion of the side shield designed on the basis of the ASOP results shown in sketch b of Fig. 9. This increase is probably due to leakage of radiation into the region from the side of the heat-pipe shield.

The dose rates in Table 6 indicate that the outer W layer in the side shield should be made slightly thicker and that other regions in the bottom shield could be trimmed or shaped. The shaping of the shield was based on isodose curves derived from the DOT calculations and plotted in Figs. 11 and 12 for neutrons and gamma rays respectively. The outer lithium hydride layer in the hemispherical (bottom) portion of the shield was trimmed back to the outer isodose curve shown in Fig. 11 and the corner formed at the junction of the hemisphere and cone was smoothed out. It was noted that the gamma-ray isodose curves plotted in Fig. 12 did not indicate any significant scattering in the direction of the crew from the shield at the side of the reactor. Therefore, it was deemed practical to taper the outer layer of W to its endpoint. The final configuration (the optimized shield) with its weight decreased to 25,589 lb is shown in Fig. 13.

Dose rates for the 100-ft radius obtained from a DOT calculation for this final configuration are given in Table 7 and isodose plots are shown in Figs. 14 and 15.* Here the dose rate at 40 deg exceeds the low-dose constraint of 3 mrem/hr and the dose rate at 150 deg is still slightly in excess of the dose constraint of 300 mrem/hr; however, all other dose rates are well below

*It will be noted that in Figs. 14 and 15 the various shield layers are outlined by stepped intervals representing the actual DOT geometry rather than by the smooth curves shown in Figs. 11 and 12. In these later figures the layers were drawn on the machine plotter, whereas in the earlier figures they were drawn by hand.

ORNL-DWG 71-4020

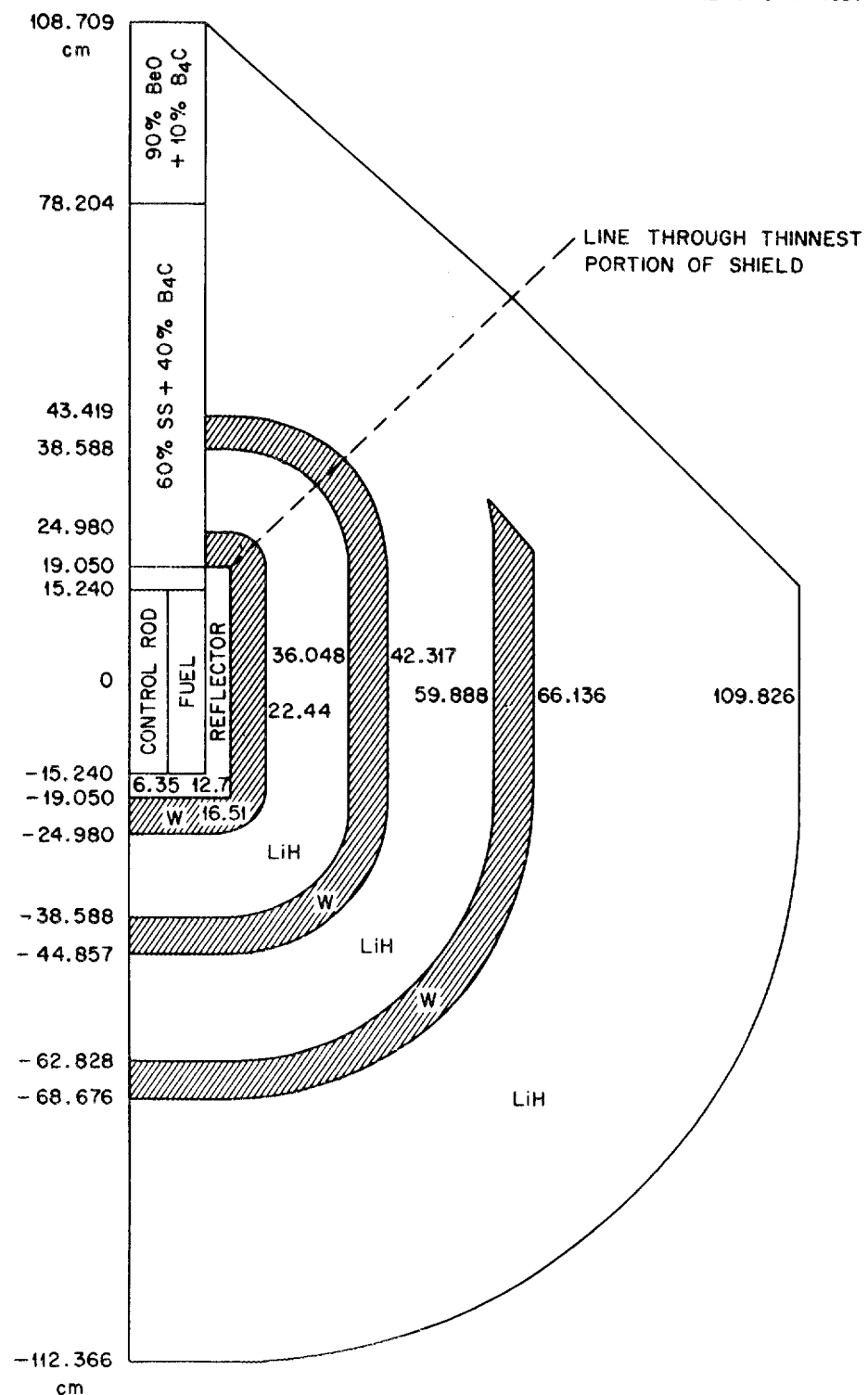


Fig. 10. Preliminary Configuration for Asymmetric Shield with a 90-deg Cone Angle (450 kWt).

Table 6. Dose Rates at a Constant 100-ft Radius Around
the Preliminary 28,305-lb Three-Cycle Shield
with 90-deg Cone Angle^a

Angle ^a (deg)	Dose Rate (mrem/hr)
0	2.38
15	2.68
30	2.57
40	2.45
60	7.17
90	28.3
120	191.0
150	339.
180	211.

^aMeasured from reactor-crew axis at center of core.

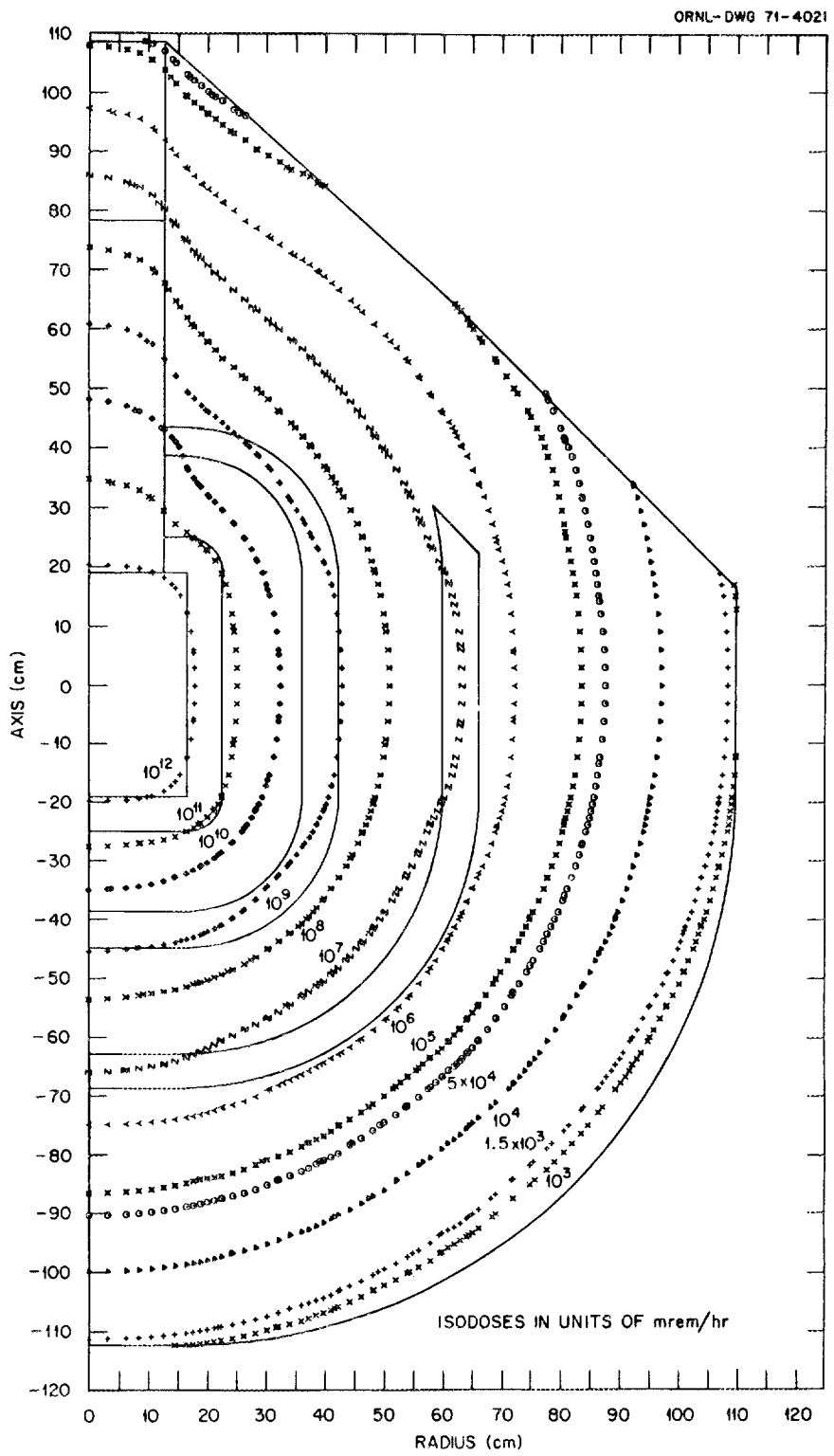


Fig. 11. Neutron Isodose Plots for Preliminary Asymmetric Shield with a 90-deg Cone Angle.

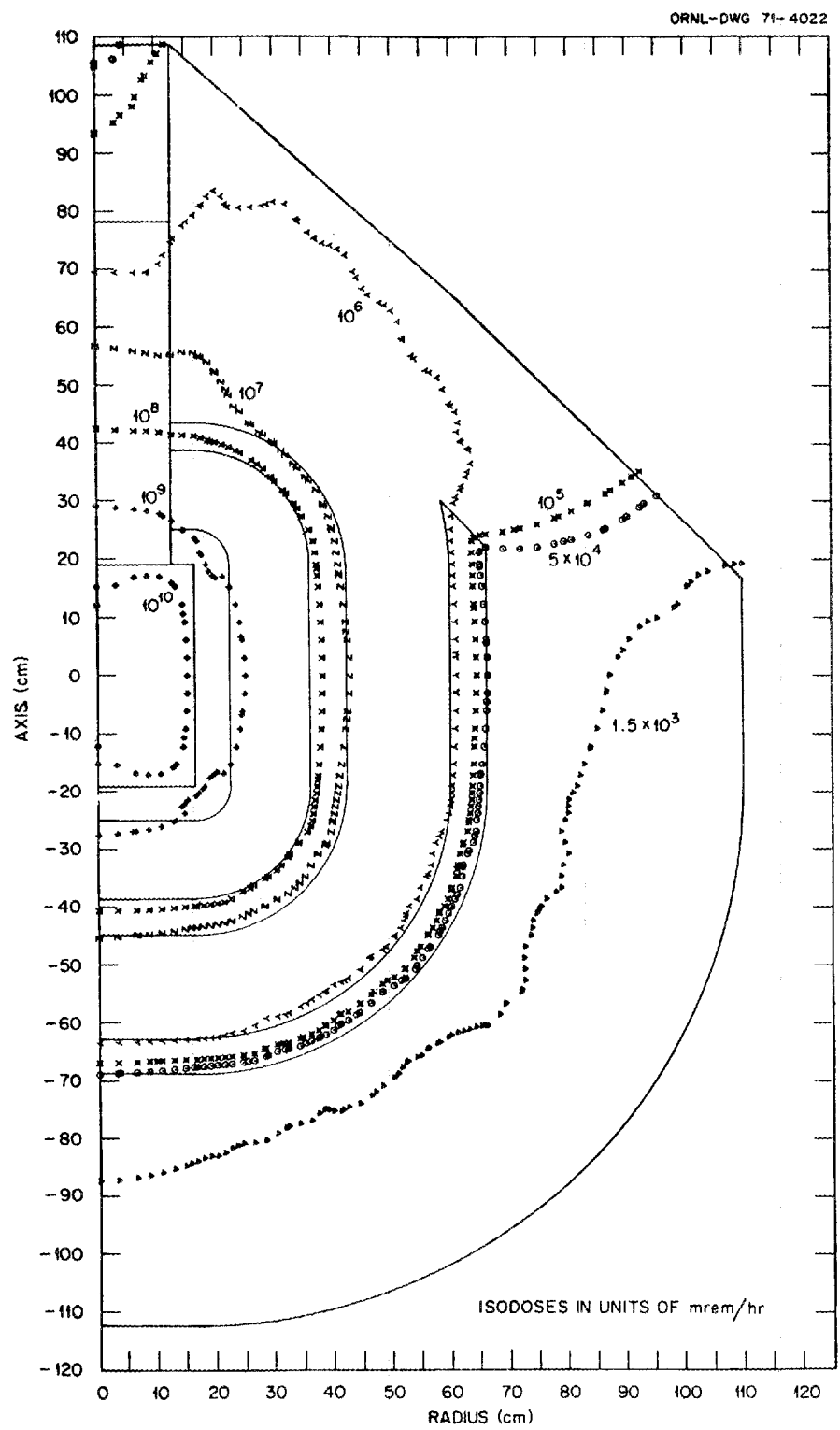


Fig. 12. Gamma-Ray Isodose Plots for Preliminary Asymmetric Shield with a 90-deg Cone Angle.

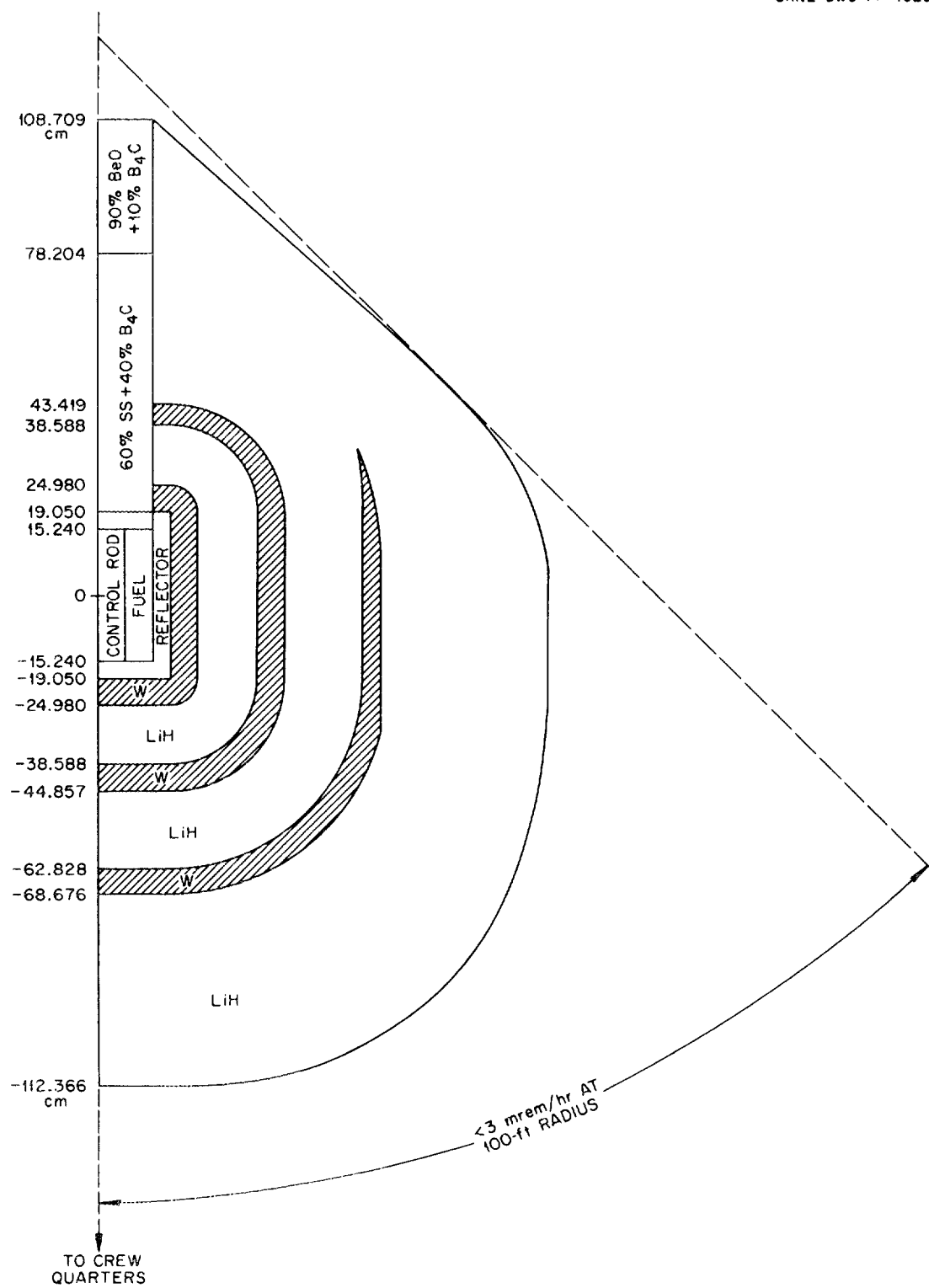


Fig. 13. Optimized Asymmetric Shield with a 90-deg Cone Angle (450 kWt).

Table 7. Dose Rates at a Constant 100-ft Radius Around
 Optimized 25,589-lb Three-Cycle Shield with
 90-deg Cone Angle^a

Angle ^a (deg)	Dose Rate (mrem/hr)		
	Total	Neutrons	Gamma Rays
0	2.30	0.57	1.73
15	2.39	0.508	1.88
30	2.81	0.638	2.17
40	3.90	0.855	3.04
60	11.66	2.32	9.35
90	32.9	5.95	26.9
120	164.	21.1	143.
150	304.	32.4	271.
180	202	36.2	165.2

^aMeasured from reactor-crew axis at center of core.

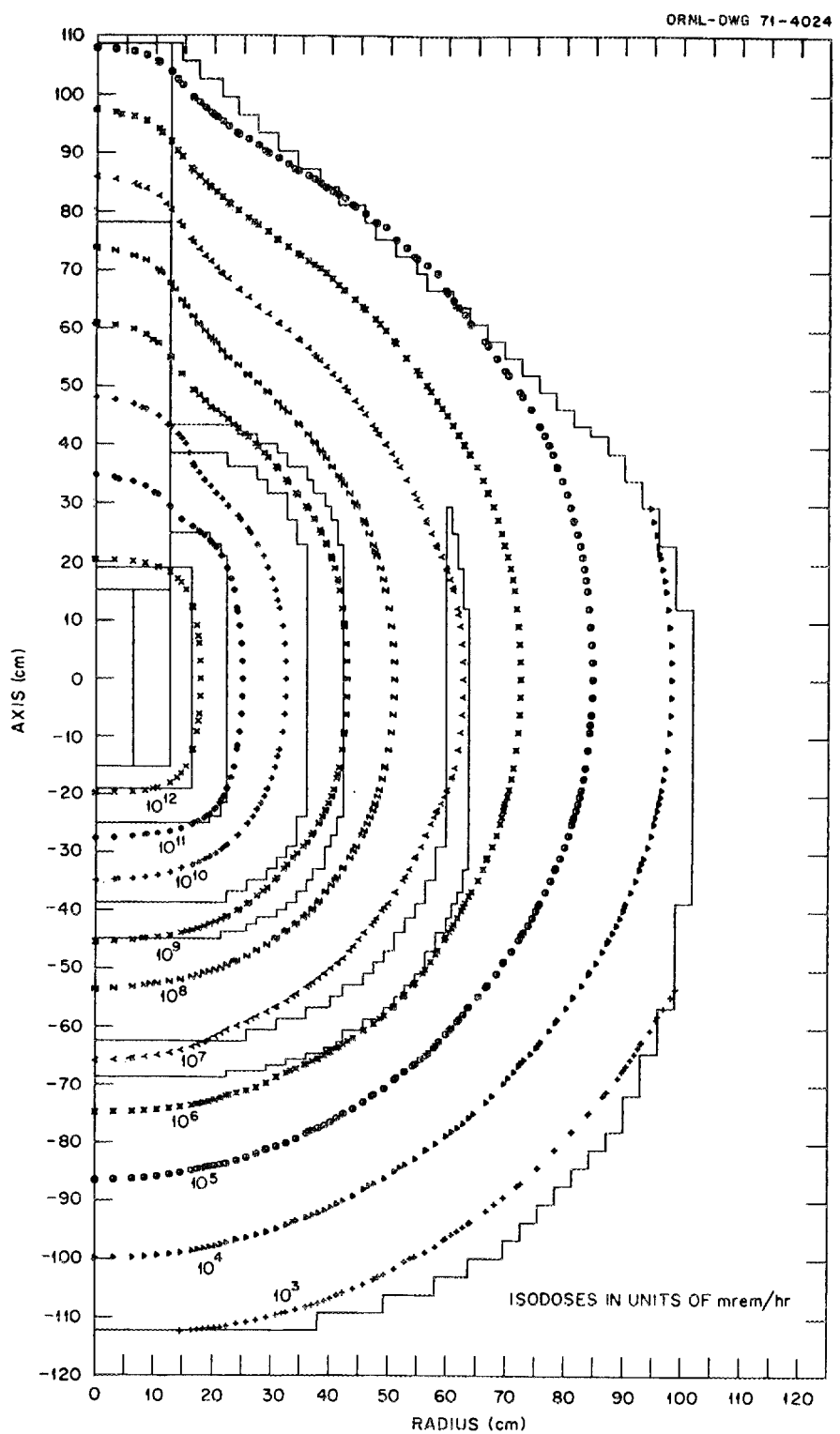


Fig. 14. Neutron Isodose Plots for Optimized Asymmetric Shield with a 90-deg Cone Angle.

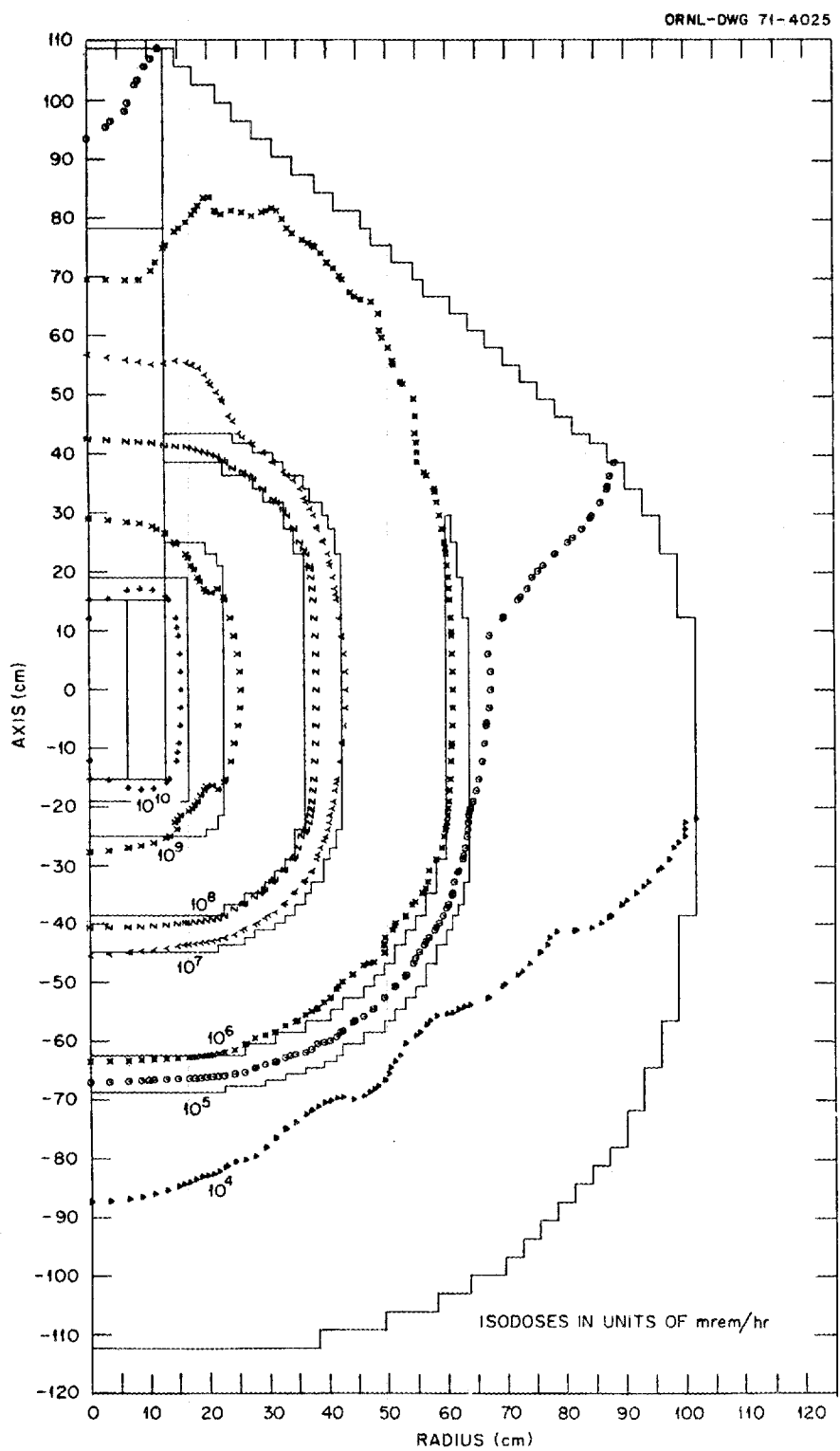


Fig. 15. Gamma-Ray Isodose Plots for Optimized Asymmetric Shield with a 90-deg Cone Angle.

the permissible levels. In particular, the total dose rate at 180 deg, that is, through the heat-pipe region, is only two-thirds the allowable dose rate and of this only 36 mrem/hr is attributable to neutrons. This low neutron dose rate is partially attributable to the effect of a low-order quadrature, S_{10} , on SPACETRAN,⁶ the computer program which transports the leakage flux from the DOT calculation to the 100-ft radius. This error is usually about a factor of two, and a biased quadrature must be used to get an accurate answer to this case.

Since the heat-pipe-cooled reactor is still in the conceptual stage, further shield shaping and additional DOT calculations were not performed in this study. It can be stated, however, that for the dose constraints and power level assumed here a shield weight between 25,000 and 26,000 lb is realistic.

APPENDIX A. SHIELD CALCULATIONS FOR HIGH-POWER OPERATION

At the time the calculations for the two-cycle shield described in Section IV were being performed, some consideration was being given by the reactor designers to operating the heat-pipe-cooled fast reactor at powers up to 1780 kWt. Some calculations for a 1780-kWt operation have been performed and are included here to illustrate the increases in shield thicknesses that can be expected with an increased reactor power.

The calculations for the higher power included survey-type ASOP calculations for a two-cycle W-LiH shield with crew dose constraints of 0.75, 3, and 12 mrem/hr at a 200-ft separation distance and calculations for a W-BeO heat-pipe region with a dose constraint of 1.2 rem/hr at a distance of 150 ft. The results, shown in Figs. A1 and A2, correspond respectively to data given in Figs. 3 and 4 for the 450-kWt operation. A comparison of Figs. 3 and A1 shows that the higher power increased the radius of the W-LiH shield approximately 12 cm for all dose constraints, and a comparison of Figs. 4 and A2 show that the radius of the heat-pipe shield was increased by about 65 cm. It is to be noted, however, that for these calculations the radius of the spherical model core itself was increased so that the volumes of the nickel control rod and fuel region were equal to those in a 14.5-in.-diam by 12-in.-high cylindrical reactor and the heat pipes comprised 50 vol% of both the core and the shield region through which they penetrated (refer to Table 2).

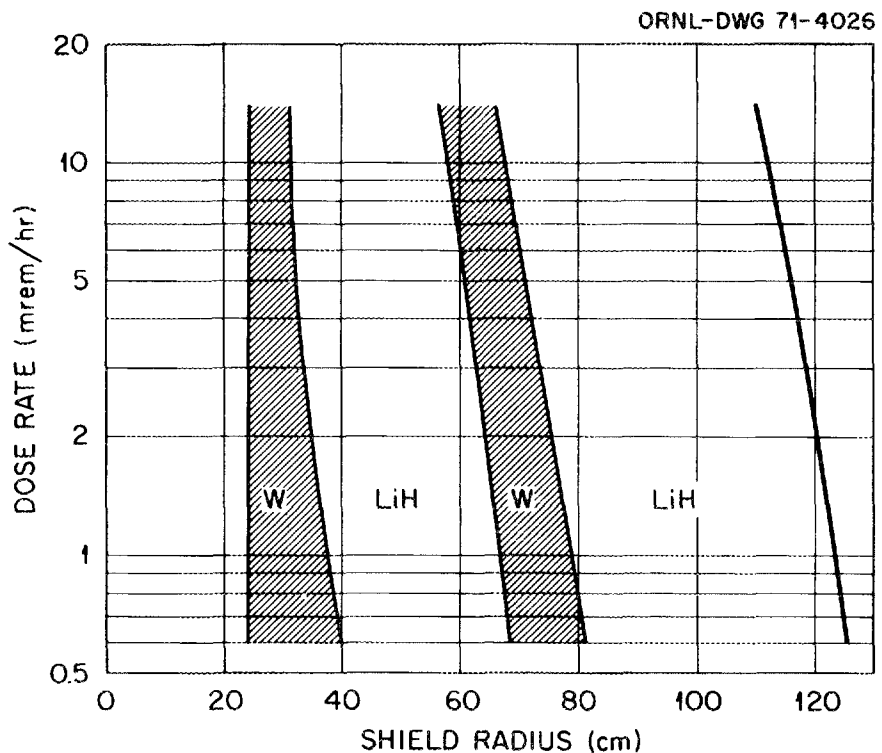


Fig. A1. Thicknesses of W and LiH Layers in a Two-Cycle Shield as a Function of Dose Rate at a Distance of 200 ft (1780 kWt).

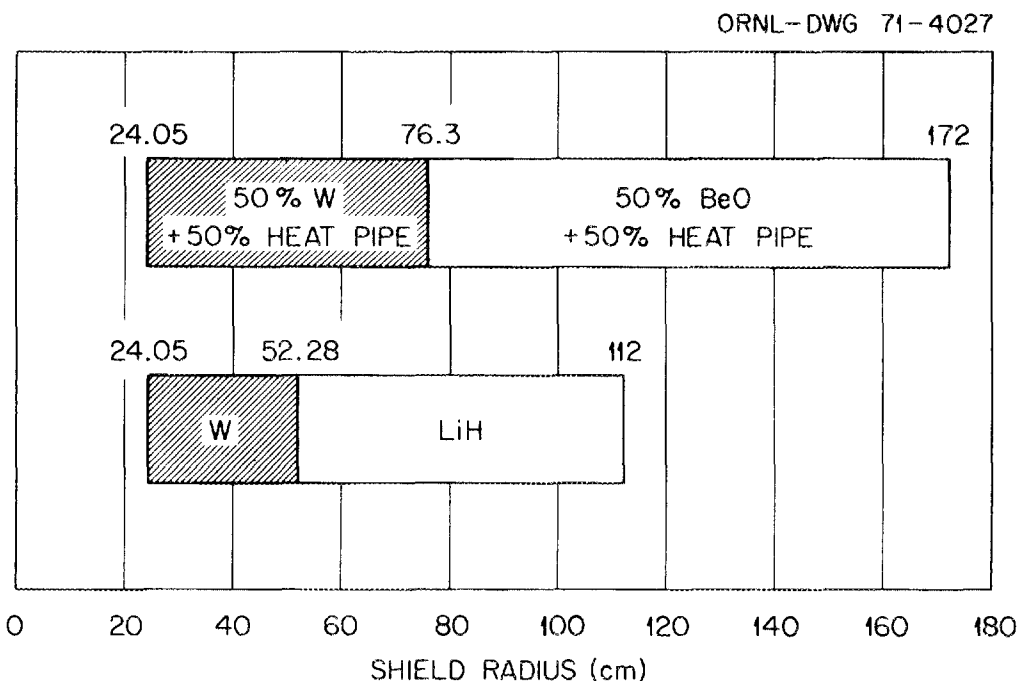


Fig. A2. Relative Thicknesses of Two Heat-Pipe Shield Configurations for a Dose Constraint of 1.2 rem/hr at a Distance of 150 ft (1780 kWt).

APPENDIX B. CROSS SECTIONS USED IN CALCULATIONS

The cross sections used in both the ASOP and the DOT calculations are contained in a 39-group library consisting of 21 neutron groups and 18 gamma-ray groups and having the energy structure shown in Table B1. The gamma-ray cross sections were obtained with the MUG program,⁷ and the neutron cross sections were mostly from an ORNL-updated version of the GAM-II library.⁸ The updated version includes some cross sections from the Evaluated Nuclear Data File (ENDF/B data).

The neutron cross sections for ^6Li and ^7Li were not taken from the GAM-II library but instead were those used by N. M. Greene⁹ in ANISN calculations of neutron transport through large thicknesses of LiH. Greene prepared the cross sections in multigroup form from a set of the latest point cross sections collected by F. Kam and F. Clark¹⁰ for a Monte Carlo calculation of neutron transport in LiH. The good agreement of the spherical ANISN calculation and a corresponding Monte Carlo calculation, plus the agreement of the results from a Monte Carlo calculation using the same cross sections with the data from the TSF SNAP-2 shadow shield experiment,¹² validated the Li cross sections used in all the calculations. Further validation was obtained when Mynatt *et al.*¹³ used the cross sections in DOT calculations that successfully predicted the penetration of neutrons through 6- and 12-in. LiH slab shields adjacent to the TSF-SNAP reactor.¹³

While the neutron cross sections for the other principal shielding material, W, were those included in the GAM-II library, they too were validated in a separate study prior to their use in these calculations. For W the most important neutron interactions are those producing gamma rays, and the cross sections for these interactions were checked by comparing calculated and measured gamma-ray spectra for this material.¹⁰

Table B1. Cross-Section Energy Group Structure

Group	Upper Energy (eV)
<u>Neutrons</u>	
1	1.4918(+7)*
2	1.0000(+7)
3	6.7032(+6)
4	4.4033(+6)
5	3.0119(+6)
6	2.0190(+6)
7	1.3534(+6)
8	9.0718(+5)
9	5.5023(+5)
10	3.3373(+5)
11	2.0242(+5)
12	1.2277(+5)
13	4.0867(+4)
14	1.1709(+4)
15	3.3546(+3)
16	7.4852(+2)
17	1.6702(+2)
18	3.7266(+1)
19	8.3153(0)
20	1.8554(0)
21	4.1399(-1)
<u>Gamma Rays</u>	
22	1.0000(+7)
23	8.0000(+6)
24	7.0000(+6)
25	6.0000(+6)
26	5.0000(+6)
27	4.0000(+6)
28	3.5000(+6)
29	3.0000(+6)
30	2.5000(+6)
31	2.0000(+6)
32	1.6000(+6)
33	1.2000(+6)
34	9.0000(+5)
35	6.0000(+5)
36	4.0000(+5)
37	2.1000(+5)
38	1.2000(+5)
39	7.0000(+4)

*Read: 1.4918×10^7 .

REFERENCES

1. W. W. Engle, Jr., "A Users Manual for ASOP, ANISN Shield Optimization Program," Union Carbide Corp., Nuclear Division, CTC-INF-941 (1969).
2. F. R. Mynatt, F. J. Muckenthaler, and P. N. Stevens, "Development of Two-Dimensional Discrete Ordinates Transport Theory for Radiation Shielding," Union Carbide Corp., Nuclear Division, CTC-INF-952 (1969).
3. A. P. Fraas, M. E. LaVerne, G. Samuels, and J. J. Tudor, "Conceptual Design of a Series of Nuclear Power Plants Employing Heat-Pipe-Cooled Reactors," ORNL-TM-2804 (1971).
4. See, for example, "Shield Design Study for a Space Station Concept," by F. R. Mynatt, W. W. Engle, Jr., and L. R. Williams, in Neutron Phys. Div. Ann. Prog. Rep. May 31, 1969, ORNL-4433, p. 64; a more complete description of this and other ASOP applications will be published later.
5. Private communication from O. L. Smith, Reactor Division, Oak Ridge National Laboratory.
6. See ref. 2, p. 80.
7. J. R. Knight and F. R. Mynatt, "MUG: A Program for Generating Multi-group Photon Cross Sections," Union Carbide Corp., Nuclear Division, CTC-17 (Jan. 20, 1970).
8. G. D. Joanou and J. S. Dudek, "GAM-II: A B₃ Code for the Calculation of Fast-Neutron Spectra and Associated Multigroup Constants," GA-4265 (1963).
9. N. M. Greene, "Multigroup ⁶Li and ⁷Li Cross Sections," in Neutron Phys. Div. Ann. Prog. Rep. May 31, 1967, ORNL-4134, p. 71.
10. F. B. K. Kam and F. H. S. Clark, "Fission Spectrum Neutron Dose Rate Attenuation and Gamma-Ray Exposure Dose Buildup Factors," Nucl. Appl. 3(7), 433 (1967).
11. W. E. Ford III and D. H. Wallace, "Discrete Ordinates Calculation of Secondary Gamma-Ray Spectra for Comparison with Tower Shielding Experiments," in Neutron Phys. Div. Ann. Prog. Rep. May 31, 1969, ORNL-4433, p. 48.

12. V. R. Cain and K. D. Franz, "Comparison of Monte Carlo Calculations with Measurements of Fast-Neutron Dose Transmitted from a Beam Source Through a SNAP-2 LiH Shield," ORNL-2423 (1968).
13. F. R. Mynatt, M. L. Gritzner, and R. J. Rodgers, "Comparisons of Discrete-Ordinates Calculations with Neutron and Gamma-Ray Slab Transmission Data for the TSF-SNAP Reactor," Neutron Phys. Div. Ann. Prog. Rep. May 31, 1969, p. 31 in ORNL-4433.

INTERNAL DISTRIBUTION

1-3.	L. S. Abbott	47-51.	J. V. Pace
4.	R. G. Alsmiller, Jr.	52.	R. W. Peelle
5.	T. W. Armstrong	53.	F. G. Perey
6.	A. R. Buhl	54.	R. W. Roussin
7.	C. E. Burgart	55.	P. N. Stevens
8-13.	R. L. Childs	56.	E. A. Straker
14.	H. C. Claiborne	57.	D. Sundberg
15.	C. E. Clifford	58.	J. A. Turner
16.	M. B. Emmett	59.	J. E. White
17-22.	W. W. Engle, Jr.	60.	L. R. Williams
23.	W. E. Ford, III	61.	H. A. Wright
24-33.	A. P. Fraas	62.	E. R. Cohen (consultant)
34.	R. M. Freestone, Jr.	63.	H. Feshbach (consultant)
35.	M. L. Gritzner	64.	H. Goldstein (consultant)
36.	L. B. Holland	65.	C. R. Mehl (consultant)
37.	J. Lewin	66.	H. T. Motz (consultant)
38.	J. L. Lucius	67-68.	Central Research Library
39.	R. E. Maerker	69.	ORNL Y-12 Technical Library Document Reference Section
40.	F. C. Maienschein	70-71.	Laboratory Records
41.	B. G. McGregor	72.	Laboratory Records ORNL RC
42.	G. L. Morgan	73.	ORNL Patent Office
43.	F. J. Muckenthaler		
44-46.	F. R. Mynatt		

EXTERNAL DISTRIBUTION

74.	P. B. Hemmig, Division of Reactor Development & Technology, U. S. Atomic Energy Commission, Washington, D. C. 20545
75.	W. H. Hannum, Division of Reactor Development & Technology, U. S. Atomic Energy Commission, Washington, D. C. 20545
76.	Kermit Laughon, AEC Site Representative
77.	R. L. Detterman, Atomics International, 8900 Desota Street, Box 308, Canoga Park, Calif.
78.	J. G. Gallagher, Manager, Thermal & Nuclear Design, Westinghouse Astronuclear Laboratory, P. O. Box 10864, Pittsburgh, Pa. 15236
79.	G. A. Graves, N-2 Division, Los Alamos Scientific Laboratory, P. O. Box 1663, Los Alamos, New Mexico 87544
80.	P. G. Johnson, Space Nuclear Propulsion Office, U. S. Atomic Energy Commission, Washington, D. C. 20545
81.	I. M. Karp, Lewis Research Center, National Aeronautics & Space Administration, 21000 Brookpark Road, Cleveland, Ohio 44135
82.	C. P. McCallum, Division of Space Nuclear Systems, U. S. Atomic Energy Commission, Washington, D. C. 20545
83-84.	Division of Technical Information Extension (DTIE)
85.	Laboratory and University Division (ORO)